

# Defect-enabled electrical current leakage in ultraviolet light-emitting diodes

**Michael W. Moseley, Andrew A. Allerman, Mary H. Crawford, Jonathan J. Wierer, Jr., Michael L. Smith, Laura B. Biedermann**

Sandia National Laboratories, Albuquerque, New Mexico, USA, 87185

**Keywords** MOCVD, leakage, nanopipe, AlGaN

Electrical current leakage paths in AlGaN-based ultraviolet (UV) light-emitting diodes (LEDs) are identified using conductive atomic force microscopy. Open-core threading dislocations are found to conduct current through insulating  $\text{Al}_{0.7}\text{Ga}_{0.3}\text{N}$  layers. A defect-sensitive  $\text{H}_3\text{PO}_4$  etch reveals these open-core threading dislocations as 1-2  $\mu\text{m}$  wide hexagonal etch pits visible with optical microscopy. Additionally, closed-core threading

dislocations are decorated with smaller and more numerous nanometer-scale pits which are quantifiable by atomic-force microscopy. The performances of UV-LEDs fabricated on similar Si-doped  $\text{Al}_{0.7}\text{Ga}_{0.3}\text{N}$  templates are found to have a strong correlation to the density of these electrically conductive open-core dislocations, while the total threading dislocation densities of the UV-LEDs remain relatively unchanged.

**1 Introduction** Ultraviolet (UV) AlGaN-based light-emitters have a wide range of applications [1,2] such as biological agent detection [3], air and water purification [4], sterilization [5], and UV phototherapy [6]. Other applications include photolithography [7] and optical data storage [8]. However, external quantum efficiencies of these UV emitters remain hindered as a result of growth challenges inherent to AlGaN materials.

Heteroepitaxial growth of AlGaN-based UV emitters on sapphire substrates requires effort to realize epilayers with a low density of threading dislocations [9,10]. Many defects formed as a result of the lattice mismatch between AlN, GaN, and sapphire are known to form below-bandgap states, which act as non-radiative recombination centers and reduce internal quantum efficiency [11]. Furthermore, it has been shown that threading dislocations can function as electrical current leakage paths [12]. These leakage paths can enable charge carriers to cross the p-n junction in LEDs without radiatively recombining, can reduce device internal quantum efficiency [13], and are considered to be a significant cause of UV-LED performance loss [14].

In this study, we investigate defect-related current-leakage mechanisms in  $\text{Al}_{0.7}\text{Ga}_{0.3}\text{N}$ -based UV-LEDs. Electrically conducting open-core threading dislocations are identified to be responsible for electrical current leak-

age through  $\text{Al}_{0.7}\text{Ga}_{0.3}\text{N}$ . A rapid and simple method of detecting and quantifying these open-core dislocations is presented. Finally, the effect of these dislocations on the performance of UV-LEDs is reported.

**2 Experimental** Two Si-doped  $\text{Al}_{0.7}\text{Ga}_{0.3}\text{N}$  templates were grown simultaneously on (0001) c-plane sapphire substrates misoriented  $0.2^\circ$  toward the m-plane in a Veeco D-125 MOCVD chamber at 75 Torr. Trimethylgallium (TMG), trimethylaluminum (TMA), and ammonia were used as precursors; silane was used as the n-type dopant. The  $\text{Al}_{0.7}\text{Ga}_{0.3}\text{N}$  templates consisted of 1.3  $\mu\text{m}$  of Si-doped  $\text{Al}_{0.7}\text{Ga}_{0.3}\text{N}$  grown on a 3.75  $\mu\text{m}$  AlN buffer layer. The threading dislocation densities of the  $\text{Al}_{0.7}\text{Ga}_{0.3}\text{N}$  layers were estimated to be  $2.0\text{--}2.4 \times 10^9 \text{ cm}^{-2}$  by x-ray diffraction (XRD) using a procedure described by Lee et al. [15]. One template was set aside for subsequent 270 nm UV-LED growth, while the other template was prepared for conductive atomic-force microscopy by the overgrowth of a 1  $\mu\text{m}$  unintentionally-doped (UID)  $\text{Al}_{0.7}\text{Ga}_{0.3}\text{N}$  layer, which was confirmed to be insulating by Hall-effect characterization.

The UID-capped  $\text{Al}_{0.7}\text{Ga}_{0.3}\text{N}$  template was analyzed with both tapping-mode atomic-force microscopy (AFM) and contact-mode conductive atomic-force microscopy (CAFM). An illustration of the CAFM setup and equiva-

lent circuit is shown in Figure 1. A  $5\text{mm} \times 5\text{mm}$  area of the template surface was scribed and painted with silver conductive paste to electrically connect to the embedded conductive n-type layer. The bias between the CAFM tip and the scribed area was kept at 10V for all current maps.

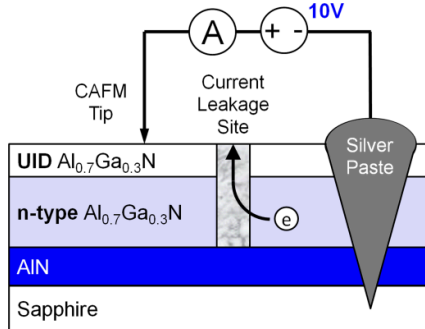


**Figure 1** Illustration and equivalent circuit of the conductive atomic-force microscope setup used to characterize the UID-capped  $\text{Al}_{0.7}\text{Ga}_{0.3}\text{N}$  template.

Pure phosphoric acid at  $160\text{ }^{\circ}\text{C}$  was used to wet etch the epitaxially-grown  $\text{Al}_{0.7}\text{Ga}_{0.3}\text{N}$  films for 60 seconds and reveal defects. AFM and optical microscopy were used to determine the effects of the acid on the morphology of the UID-capped  $\text{Al}_{0.7}\text{Ga}_{0.3}\text{N}$  template surface and to quantify the density of etch pits.

**3 Results and Discussion** Two Typical contact-mode CAFM current and height data of the as-grown UID-capped  $\text{Al}_{0.7}\text{Ga}_{0.3}\text{N}$  template are shown in Figure 2. The 50X optical microscope image in the inset depicts the same surface area measured by the CAFM height data. The current map shown in Figure 2(a) reveals a singular current transport site through the UID  $\text{Al}_{0.7}\text{Ga}_{0.3}\text{N}$  layer. The observed site of current leakage corresponded to an area of surface abnormality in the CAFM height data as indicated by the arrow in Figure 2(b), yet the same area imaged by the optical microscope appeared flat and featureless, as shown in the inset of Figure 2(b). Therefore, CAFM measurements were necessary to clearly identify current leakage sites in the as-grown  $\text{Al}_{0.7}\text{Ga}_{0.3}\text{N}$  templates.

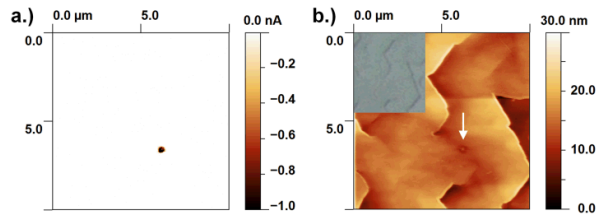


**Figure 2**  $10 \times 10 \mu\text{m}$  (a.) Contact-mode CAFM current map, (b.) CAFM height data, and (inset) 50X optical microscope image of a location on UID-capped  $\text{Al}_{0.7}\text{Ga}_{0.3}\text{N}$  template.

Electrical conduction through open-core threading dislocations has been previously observed in GaN [16]. Open-core threading dislocations (i.e. nanopipes) have been described as hollow tubes in the epitaxially-grown material [16] with inner diameters from 2 nm to 50 nm [17]. The mechanism of electrical conduction through nanopipes is still a subject of debate, but evidence suggests that impurity contamination contributes to a conductive path along the inner wall of the nanopipe [18]. Phosphoric acid [17] and other etches [19,20] have been reported to produce hexagonal pits at nanopipes in GaN by anisotropic etching along the inner walls [21].

The UID-capped  $\text{Al}_{0.7}\text{Ga}_{0.3}\text{N}$  template was then wet etched in phosphoric acid to determine if nanopipes are responsible for the observed sites of electrical current conduction. After etching, the same location of the etched UID-capped  $\text{Al}_{0.7}\text{Ga}_{0.3}\text{N}$  template that was shown in Figure 2 was re-measured (with minimal lateral offset) and is shown in Figure 3 by the contact-mode CAFM height data. The point that had previously exhibited current leakage had been etched into a  $1.1 \mu\text{m}$  wide hexagonal pit. Also shown in the inset of Figure 3 is a 50X optical microscope image of the same area where the same etch pit is clearly visible. These observations of hexagonal etch pit formation by hot phosphoric acid at sites of electrical current transport through a nominally insulating layer suggest that nanopipes are responsible for the electrical conduction through the UID  $\text{Al}_{0.7}\text{Ga}_{0.3}\text{N}$  epilayers.

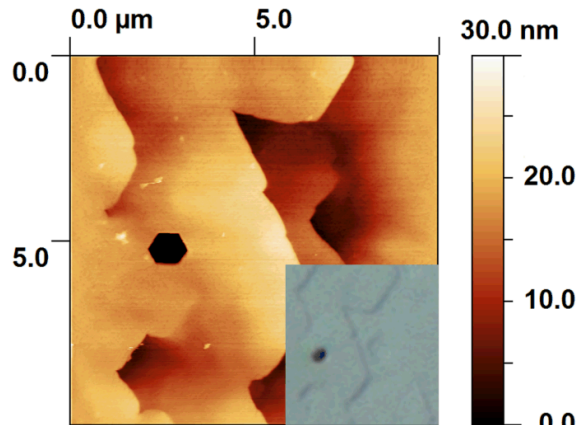


**Figure 3**  $10 \times 10 \mu\text{m}$  Contact-mode CAFM height data and (inset) optical microscope morphology of the UID-capped  $\text{Al}_{0.7}\text{Ga}_{0.3}\text{N}$  template locations shown in Figure 2 after etching in hot phosphoric acid.

With wet etching, nanopipe density can easily be quantified by optical microscopy, avoiding time-consuming CAFM measurements. Shown in Figure 4 is a 50X optical microscope image of the etched UID-capped  $\text{Al}_{0.7}\text{Ga}_{0.3}\text{N}$  template surface with a hexagonal etch pit density of  $\sim 7.5 \times 10^5 \text{ cm}^{-2}$ . The density of these nanopipes is approximately four orders of magnitude smaller than the density of

threading dislocations determined by XRD. The rapid quantification of nanopipe density by  $H_3PO_4$  etching has proven itself an effective feedback mechanism in the improvement of these  $Al_{0.7}Ga_{0.3}N$  layers. This technique has aided in the lowering of the density of nanopipes in MOCVD-grown  $Al_{0.7}Ga_{0.3}N$  layers by almost two orders of magnitude via improvements in sapphire nitridation, layer nucleation, and buffer growth conditions.

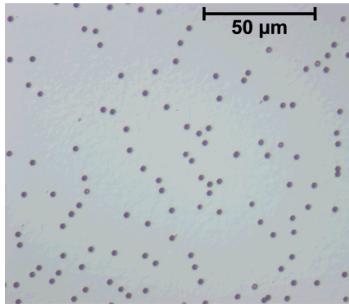


**Figure 4** Optical microscope image of an etched  $Al_{0.7}Ga_{0.3}N$  surface displaying micron-scale hexagonal etch pits with a density of  $\sim 7.5 \times 10^5 \text{ cm}^{-2}$ .

Small, nanometer-scale etch pits are also revealed by the phosphoric acid etch. A smaller,  $2 \times 2 \mu\text{m}$  tapping-mode AFM morphology of a similar area of the etched UID-capped  $Al_{0.7}Ga_{0.3}N$  template is shown in Figure 5. The average density of these pits measured at multiple locations was found to be  $2.5 \times 10^9 \text{ cm}^{-2}$ . The total threading dislocation density of the  $Al_{0.7}Ga_{0.3}N$  layers was estimated to be  $2.0$  to  $2.4 \times 10^9 \text{ cm}^{-2}$  by x-ray diffraction. Other reports have shown that  $H_3PO_4$  can selectively etch screw-, edge-, and mixed-type dislocations in GaN, yielding a close agreement with dislocation densities determined by TEM [22]. Therefore, these data suggest that  $H_3PO_4$  etching of the  $Al_{0.7}Ga_{0.3}N$  layers allows for quantification of the total threading dislocation density in addition to the nanopipe density.

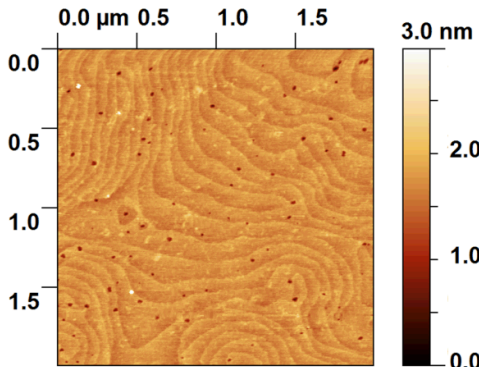


**Figure 5** Tapping-mode  $2 \times 2 \mu\text{m}$  atomic-force microscope morphology of a similar area of the etched UID-capped  $Al_{0.7}Ga_{0.3}N$  template, which shows individual threading dislocations.

The second Si-doped  $Al_{0.7}Ga_{0.3}N$  template was used for the growth and fabrication of  $300 \times 300 \mu\text{m}$  UV-LEDs with emission at  $270 \text{ nm}$ . Shown in Figure 6 are the relative output powers of LEDs with nanopipe densities measured at corresponding locations on the etched UID-capped  $Al_{0.7}Ga_{0.3}N$  template. The nanopipe densities ranged from  $4 \times 10^5 \text{ cm}^{-2}$  to  $2.1 \times 10^6 \text{ cm}^{-2}$ , which translates to 350 to 1900 per  $300 \times 300 \mu\text{m}$  device. The on-wafer UV-LED emission intensities were found to be inversely proportional to the densities of hexagonal etch pits (nanopipes). However, the total threading dislocation density varied by less than 30% over the same regions as the tested LEDs.

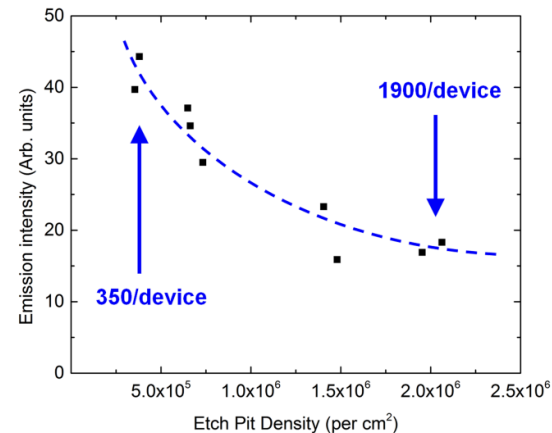


**Figure 6** Relative output powers of LEDs grown on the Si-doped  $Al_{0.7}Ga_{0.3}N$  template vs. the etch pit densities at the corresponding location on the etched UID-capped  $Al_{0.7}Ga_{0.3}N$  template.

The authors attribute this strong inverse correlation between nanopipes and UV-LED output power to electrical current leakage through open-core threading dislocations. Current transport through these nanopipes can shunt the quantum well active regions by carrying current across the p-n junction and preventing radiative recombination. These data suggest that nanopipes acting as current leakage paths can have a larger effect on LED electroluminescence independent of threading dislocations.

**4 Conclusion** Two In this study, open-core threading dislocations are observed to significantly degrade the performance of UV-LEDs while composing only a small fraction ( $<0.1\%$ ) of the total threading dislocation density. The performances of UV-LEDs grown and fabricated on Si-doped  $Al_{0.7}Ga_{0.3}N$  templates were found to have a strong inverse correlation with open-core threading dislocations while total threading dislocation densities of the  $Al_{0.7}Ga_{0.3}N$  templates remain relatively constant. These data suggest that open-core threading dislocations can limit UV-LED performance by shunting current past quantum wells and reducing internal quantum efficiencies.

Defect-related sites of electrical current leakage in  $\text{Al}_{0.7}\text{Ga}_{0.3}\text{N}$  observed by CAFM are easily decorated by  $\text{H}_3\text{PO}_4$  etching. These micron-scale etch pits were attributed to open-core threading dislocations (i.e. nanopipes). Smaller, nanometer-scale etch pits were also observed and attributed to closed-core threading dislocations. The defect-sensitive etch proved an effective feedback mechanism to determine growth conditions resulting in lower density of nanopipes.

Sandia National Laboratories is a multi-program laboratory managed and operated by Sandia Corporation, a wholly owned subsidiary of Lockheed Martin Corporation, for the United States Department of Energy's National Nuclear Security Administration under contract DE-AC04-94AL85000.

- [20] S. Lee, D. Oh, H. Goto, J. Ha, H. Lee, T. Hanada, M. Cho, T. Yao, S. Hong, and H. Lee, *Appl. Phys. Lett.* 89, 132117.(2006).
- [21] S. Hong, B. Kim, H. Park, Y. Park, S. Yoon, and T. Kim, *J. Cryst. Growth* 191, 275.(1998).
- [22] X. Xu, R. P. Vaudo, J. Flynn, and G. R. Brandes, *Journal of Elec Materi* 31, 402.(2002).

## References

- [1] M. A. Khan, *Phys. Status Solidi A* 203, 1764.(2006).
- [2] M. A. Khan, M. Shatalov, H. P. Maruska, H. M. Wang, and E. Kuokstis, *Jpn. J. Appl. Phys.* 44, 7191.(2005).
- [3] Q. Li, P. K. Dasgupta, H. Temkin, M. H. Crawford, A. J. Fischer, A. A. Allerman, K. H. A. Bogart, and S. R. Lee, *Appl. Spectrosc.* 58, 1360.(2004).
- [4] S. Vilhunen, H. Särkkä, and M. Sillanpää, *Environ Sci Pollut Res* 16, 439.(2009).
- [5] Y. Bilenko, A. Luney, X. Hu, J. Deng, T. M. Katona, J. Zhang, R. Gaska, M. S. Shur, W. Sun, V. Adivarahan, M. Shatalov, and A. Khan, *Jpn. J. Appl. Phys.* 44, L98.(2005).
- [6] P. Hart, S. Gorman, and J. Finlay-Jones, *Nat. Rev. Immunol.* 11, 584.(2011).
- [7] G. Roelkens, P. Dumon, W. Bogaerts, D. Van Thourhout, and R. Baets, *IEEE Photonic Tech. L.* 17, 2613.(2005).
- [8] S. Abe, S. Sato, E. Ito, M. Tsukuda, M. Tomiyama, and E. Ohno, *Jpn. J. Appl. Phys.* 41, 1704.(2002).
- [9] H. Hirayama, T. Yatabe, N. Noguchi, T. Ohashi, and N. Kamata, *Appl. Phys. Lett.* 91, 071901.(2007).
- [10] O. Reentilä, F. Brunner, A. Knauer, A. Mogilatenko, W. Neumann, H. Protzmann, M. Heuken, M. Kneissl, M. Weyers, and G. Tränkle, *J. Cryst. Growth* 310, 4932.(2008).
- [11] A. Touhidul Islam, N. Murakoshi, T. Fukuda, H. Hirayama, and N. Kamata, *Phys. Status Solidi C* 11, 832.(2014).
- [12] J. S. Speck and S. Rosner, *Physica B* 273, 24.(1999).
- [13] M.-H. Chang, D. Das, P. Varde, and M. Pecht, *Microelectron. Reliab.* 52, 762.(2012).
- [14] R. Jiang, D. Yan, H. Lu, R. Zhang, D. Chen, and Y. Zheng, *Chinese Sci. Bull.* 59, 1276.(2014).
- [15] S. R. Lee, A. M. West, A. A. Allerman, K. E. Waldrip, D. M. Follstaedt, P. P. Provencio, D. D. Koleske, and C. R. Abernathy, *Appl. Phys. Lett.* 86, 241904.(2005).
- [16] D. Cherns and M. Hawkridge, *J. Mater. Sci.* 41, 2685.(2006).
- [17] S. Hong, T. Yao, B. Kim, S. Yoon, and T. Kim, *Appl. Phys. Lett.* 77, 82.(2000).
- [18] R. Jones, J. Elsner, M. Haugk, R. Gutierrez, T. Frauenheim, M. Heggie, S. Öberg, and P. Briddon, *Phys. Status Solidi A* 171, 167.(1999).
- [19] G. Kamler, J. Weyher, I. Grzegory, E. Jezierska, and T. Wosiński, *J. Cryst. Growth* 246, 21.(2002).